

## Highly birefringent colloidal particles for tracer studies

This article has been downloaded from IOPscience. Please scroll down to see the full text article.

2004 J. Phys.: Condens. Matter 16 S4137

(<http://iopscience.iop.org/0953-8984/16/38/027>)

View [the table of contents for this issue](#), or go to the [journal homepage](#) for more

Download details:

IP Address: 129.252.86.83

The article was downloaded on 27/05/2010 at 17:46

Please note that [terms and conditions apply](#).

## Highly birefringent colloidal particles for tracer studies

**K Sandomirski, S Martin, G Maret, H Stark and T Gisler**

Universität Konstanz, Fachbereich Physik, D-78457 Konstanz, Germany

Received 21 May 2004, in final form 20 July 2004

Published 10 September 2004

Online at [stacks.iop.org/JPhysCM/16/S4137](http://stacks.iop.org/JPhysCM/16/S4137)

doi:10.1088/0953-8984/16/38/027

### Abstract

We report on the preparation and characterization of highly birefringent, monodisperse colloidal particles with sizes between 100 nm and some micrometres made by emulsification of a reactive acrylate monomer in aqueous solution. Photopolymerization of the emulsion droplets in the liquid crystalline state results in particles with frozen orientational order. Particles that had not been polymerized have a higher effective birefringence than the polymerized particles at room temperature, as shown by measurements of the depolarized scattering intensity using quasi-elastic light scattering (QELS). We also present preliminary results showing that larger particles can be made to rotate with optical tweezers with circular polarization.

The presence of hydrodynamic interactions (HI) in colloidal suspensions and polymer solutions leads to qualitatively new phenomena that are not found in simple liquids. Examples are the equilibrium dynamics and the flow behaviour of dense colloidal suspensions [1–3]. When a colloidal particle moves due to the random forces imparted by the surrounding fluid molecules, it excites a flow field that transfers linear momentum to surrounding particles. The flow field due to a translating particle is inhomogeneous, which results in neighbouring particles experiencing a torque. Similarly to this coupling of rotation and translation, the flow field excited by the Brownian rotation of a colloidal particle can transfer angular momentum to neighbouring particles, leading to rotation–rotation coupling.

While detailed insight on the influence of HI on the translational degrees of freedom in colloidal suspensions has been obtained from quasi-elastic light scattering (QELS) and real-space imaging experiments, much less is known about the effect of HI on the rotational motion. Rotational motion can be observed in depolarized quasi-elastic light scattering experiments on optically anisotropic particles [4, 5], using time-resolved phosphorescence anisotropy measurements on specially labelled particles [6], or nuclear magnetic resonance [7]. Measured autocorrelation functions of the scattered electric field measured by depolarized QELS now contain information not only on the particle displacements but also on their

orientations. Using index-matched colloidal Teflon particles, Degiorgio *et al* measured the rotational diffusion coefficient  $D_r(\phi)$  at volume fractions  $\phi$  as high as 0.5 [4]. Theoretical predictions for  $D_r(\phi)$  in concentrated suspensions have been worked out, similar to the case of the translational diffusion coefficient, by configuration space and ensemble averages of products of pair correlation functions and mobility tensors. Experimental data show that at short times rotation and translation decouple. At longer times, experimental orientational correlation functions deviate from the predictions of the decoupling approximation, indicating that translation–rotation coupling becomes increasingly important.

In order to test theories that go beyond the decoupling approximation, the simultaneous real-space observation of particle positions and orientations could pave the way to a detailed understanding of the role of HI on rotational diffusion in colloidal suspensions. Measuring particle orientations in a polarization microscope requires that the particles possess a sufficiently high birefringence that a rotation of the particle director leads to a measurable change in the transmitted intensity under crossed polarizers.

At present, there are three classes of spherical, birefringent colloidal particles available: (i) fluoropolymer latex particles, (ii) inorganic particles, and (iii) particles made by emulsification of liquid crystals.

Among the fluoropolymer particles, the ones made of polytetrafluoroethylene (PTFE) were reported to have a relatively high birefringence ( $\Delta n \approx 0.04$ ) due to their high crystallinity [8]. However, they are rod-like rather than spherical. Particles made of copolymers of tetrafluoroethylene and perfluoroalkyl–perfluorovinylethers (PFA) [8] have a birefringence  $\Delta n \approx 0.005$  [9] due to their low crystallinity. However, both PTFE and PFA particles discussed in the literature have diameters which are too small to allow them to be observed directly in a polarization microscope.

Inorganic materials, on the other hand, often have high birefringence in the crystalline state. Spherical colloidal particles prepared via sol–gel reactions are, however, mostly polycrystalline. A notable exception is spherical crystalline particles of the calcium carbonate vaterite [10], which can be grown up to several micrometres in diameter, sufficient for a high light transmission through crossed polarizers.

The third class of optically anisotropic colloids is liquid crystal emulsions which can be prepared by extrusion into a co-flowing liquid stream [11], resulting in highly monodisperse particles with sizes from some tens to hundreds of micrometres.

Polymerizing liquid crystal emulsion droplets made of a nematogenic acrylate precursor was shown to produce highly birefringent particles some tens of micrometres in diameter [12]. The value of the birefringence of these particles is not known, but it is high enough to produce clear Maltese cross patterns under crossed polarizers. It is, however, not clear whether sub-micrometre sized polymerized liquid crystalline particles would have sufficient birefringence that they could be useful for real-space tracer experiments.

In the present publication we report on a new type of birefringent colloidal particles suited for the real-space study of rotational Brownian motion, namely unpolymerized particles of the acrylate precursor cooled below the crystalline–nematic (C–N) transition temperature. By adjustment of the preparation parameters, monodisperse particles with diameters between 100 nm and about 1  $\mu\text{m}$  can be prepared reproducibly. Characterization by quasi-elastic light scattering and magnetic birefringence shows that these unpolymerized particles have a higher birefringence than the polymerized ones. Finally, we report on an implementation of an optical tweezer setup that allows for the observation and control of the position and orientation of such birefringent particles.

We synthesize birefringent particles by a procedure similar to, but slightly different from, the one by Cairns *et al* [12]. We dissolve reactive monomer RM257 (EM Industries) and

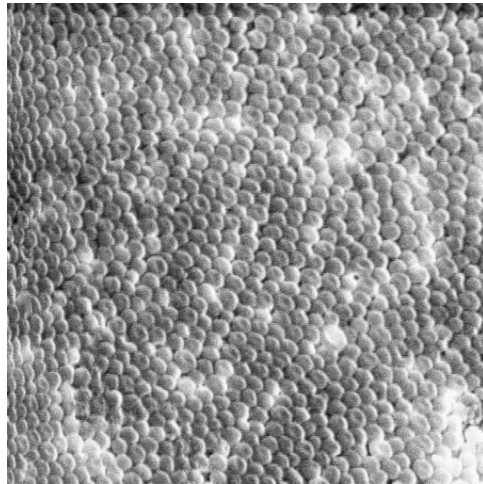


**Figure 1.** Scanning electron micrograph of polymerized mesogen particles with diameter  $2R \sim 800$  nm produced by emulsification of a mixture of RM257 with photoinitiator. The crystallization of the particles indicates low size polydispersity.

the photoinitiator Darocur 1173 (Ciba) into ethanol at  $50^\circ\text{C}$ . The solution containing the dissolved acrylate precursor at weight concentrations between  $10^{-4}$  and  $10^{-3}$  is then added drop by drop into an ethanol–water mixture kept at  $70^\circ\text{C}$ , slightly above the crystal–nematic transition temperature  $T_{\text{CN}} = 68^\circ\text{C}$  of RM257. The dissolution of the ethanol from the drops into the water phase leads to a precipitation of the mesogen, resulting in droplets with nematic order in the size range from about 100 nm to some microns.

Two different protocols are then followed. In the first, the particles are polymerized by irradiating the solution with UV light, which results in a ‘locking’ of the nematic order, after which the suspension is cooled down slowly to room temperature. In the second protocol, the precursor is emulsified as above, but without the photoinitiator, and is then slowly cooled to room temperature.

Figure 1 shows a scanning electron micrograph of polymerized nematic particles. Here the size polydispersity (typically between 7% and 12%) was reduced by gentle centrifugation of the crude suspension to a level low enough that the particles crystallize. We find that the particle size is mainly determined by the rate of evaporation of the ethanol: high evaporation rates lead to small particles, while slow evaporation over days leads to large particles. Using a given set of preparation parameters (ethanol–water mixing ratio, ethanol evaporation rate) we are able to reproduce average particle sizes between different preparations to within about 5%.

Static light scattering shows that both the polarized and depolarized scattering intensity  $I_{\text{VV}}(q)$  and  $I_{\text{VH}}(q)$  decay monotonically with scattering wavevector  $q$  (see figure 2). The polarized scattering due to the mismatch of the refractive indices of the particle and of the solvent is about 50–100 times larger than the depolarized intensity which originates in the birefringence of the particle. The ordinary refractive index  $n_{\perp} = 1.55$  of the bulk material in the nematic phase at  $T = 70^\circ\text{C}$  leads us to expect that in water the scattering from these particles is no longer described by Rayleigh–Gans, but rather by Mie theory [13]. Unfortunately, however, Mie solutions for birefringent particles are not known, and one has to resort to numerical methods such as the discrete-dipole approximation (DDA) [14] for a detailed understanding of measured scattering intensities in terms of the liquid crystal director configuration and the

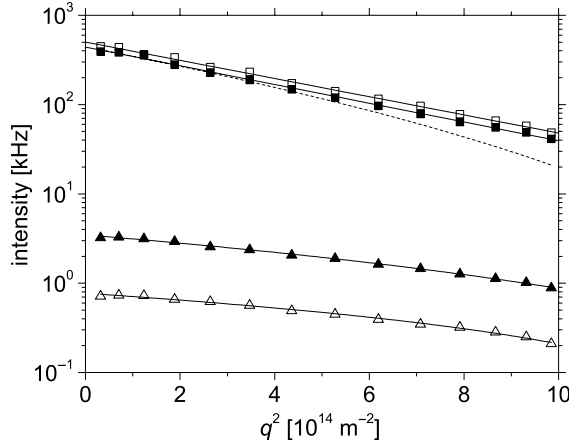


**Figure 2.** Polarized and depolarized scattering intensities  $I_{VV}(q)$  (squares) and  $I_{VH}(q)$  (triangles) of polymerized (open symbols) and unpolymerized (full symbols) mesogen particles as a function of scattering wavevector  $q$ . Full lines are fits of the function  $\ln(I(q)/I(q=0)) = 1 - Aq^2 + Bq^4$  to the data. The particle radius  $R = 110$  nm obtained from a fit to  $I_{VV}(q)$  using  $A = R^2/5$  [17] is, given the size polydispersity of about 10%, in good agreement with the hydrodynamic radius  $R_h = 100$  nm measured by quasi-elastic light scattering (data not shown). The broken curve is the Rayleigh-Gans form factor  $P(q) = [3(\sin(qR) - qR \cos(qR))/(qR)^3]^2$  for monodisperse, optically isotropic spheres, scaled to  $I_{VV}(q=0)$ .

intrinsic birefringence of the liquid crystal, in particular when the particle sizes are comparable with the wavelength of light. In the following we will restrict our discussion to particle sizes  $R < 100$  nm for which Rayleigh-Gans theory is still a good approximation.

When the photoinitiator and the UV curing step are omitted in the particle preparation, the polarized scattering intensity  $I_{VV}(q)$  measured in static light scattering shows an angular dependence which is very similar to the one of  $I_{VV}(q)$  from polymerized particles. However, the depolarized intensity  $I_{VH}(q)$  of unpolymerized particles is now by a factor of five higher than for polymerized nematic particles, in contrast to the polymerization-induced birefringence increase of main-chain nematics. This reflects a reduction of the birefringence upon polymerization which could be due to polymerization-induced director field distortions.

In order to determine the effective birefringence of the particles, we calculate the orientationally averaged  $I_{VV}(q)$  and  $I_{VH}(q)$  within the Rayleigh-Gans approximation [15]. We assume that the local dielectric constant  $\varepsilon_{ij}(\mathbf{r})$  at the position  $\mathbf{r}$  within the particle can be described by the uniaxial form

$$\varepsilon_{ij}(\mathbf{r}) = \varepsilon_{\perp} \delta_{ij} + \Delta \varepsilon v_i(\mathbf{r}) v_j(\mathbf{r}) \quad (1)$$

where  $\Delta \varepsilon = \varepsilon_{\parallel} - \varepsilon_{\perp}$  is the anisotropy in the dielectric constant of the bulk material, and  $v_i(\mathbf{r})$  is the  $i$ th Cartesian component of the local nematic director  $\mathbf{v}(\mathbf{r}) = (\sin \vartheta(\mathbf{r}) \cos \varphi(\mathbf{r}), \sin \vartheta(\mathbf{r}) \sin \varphi(\mathbf{r}), \cos \vartheta(\mathbf{r}))$  oriented with polar angles  $\vartheta(\mathbf{r})$  and  $\varphi(\mathbf{r})$  with respect to the average particle director  $\mathbf{u}$ . The dielectric constants  $\varepsilon_{\parallel}$  and  $\varepsilon_{\perp}$  are related to the ordinary and extraordinary refractive indices  $n_{\perp}$  and  $n_{\parallel}$  of the bulk material by  $n_{\parallel}^2 = \varepsilon_{\parallel}$  and  $n_{\perp}^2 = \varepsilon_{\perp}$ .

Following the treatment in [16], we have calculated the Rayleigh-Gans scattering from nematic particles suspended in a solvent of dielectric constant  $\varepsilon_s$  [15]. The depolarization ratio

$I_{\text{VH}}(q)/I_{\text{VV}}(q)$  at  $q = 0$  can be written as

$$\frac{I_{\text{VH}}(q = 0)}{I_{\text{VV}}(q = 0)} = \frac{(\Delta\tilde{\varepsilon})^2}{15(\tilde{\varepsilon}_{\perp} - \varepsilon_s)^2 + 10(\tilde{\varepsilon}_{\perp} - \varepsilon_s)\Delta\tilde{\varepsilon} + 3(\Delta\tilde{\varepsilon})^2}. \quad (2)$$

Averaging over the inhomogeneous orientation of the director  $\boldsymbol{v}(\boldsymbol{r})$  within the particle results in an effective ordinary dielectric constant

$$\tilde{\varepsilon}_{\perp} = \varepsilon_{\perp} + \Delta\varepsilon \frac{3}{4\pi R^3} \int d^3\boldsymbol{r} \sin^2 \vartheta(\boldsymbol{r}) \cos^2 \varphi(\boldsymbol{r}), \quad (3)$$

which may be larger than the bulk ordinary dielectric constant. Conversely, an inhomogeneous director field leads to an effective dielectric anisotropy

$$\Delta\tilde{\varepsilon} = \Delta\varepsilon \left[ 1 - \frac{9}{8\pi R^3} \int d^3\boldsymbol{r} \sin^2 \vartheta(\boldsymbol{r}) \right], \quad (4)$$

which may be smaller than the bulk dielectric anisotropy.

Using equation (2) and the measured depolarization ratio  $I_{\text{VH}}(q = 0)/I_{\text{VV}}(q = 0) = 8.69 \times 10^{-3}$  for the unpolymerized particles we obtain an effective birefringence  $\Delta\tilde{n} = 2\tilde{\varepsilon}_{\perp}\Delta\tilde{\varepsilon} + (\Delta\tilde{\varepsilon})^2 = 0.083$ , approximating the effective ordinary dielectric constant  $\tilde{\varepsilon}_{\perp}$  by its bulk value  $n_{\perp}^2 = 2.40$ . This value is in good agreement with the value  $\Delta n = 0.13$  obtained from measurements of the magnetic birefringence on a highly dilute suspension. These values for the birefringence are considerably lower than the estimated value  $\Delta n \approx 0.2$  for the bulk liquid crystal, indicating a lower orientational order than in the bulk nematic phase. Compared to the unpolymerized particles, the polymerized particles have a much smaller effective birefringence ( $\Delta\tilde{n} = 0.031$ ), reflecting a significant perturbation of the nematic order in the particle due to the polymerization process.

The fact that the particles' size is small, but not negligible, compared to the wavelength of light gives rise to a decrease of both polarized and depolarized scattering intensities with increasing scattering wavevector  $q$  (see figure 2). In the Guinier regime where  $qR < \sqrt{5}$ , Rayleigh–Gans theory for nematic particles predicts a behaviour

$$I_{\text{VV}}(q)/I_{\text{VV}}(q = 0) = 1 - c_{\text{VV}}(qR)^2/5 + \mathcal{O}((qR)^4) \quad (5)$$

for the polarized scattering intensity, similar to the Guinier law  $I_{\text{VV}}(q) \sim \exp(-(qR)^2/5) \approx 1 - (qR)^2/5$  for optically isotropic particles. The prefactor  $c_{\text{VV}}$  depends on the internal director field; for a homogeneous director field  $c_{\text{VV}} = 1$  [15].

The depolarized scattering intensity  $I_{\text{VH}}(q)$  predicted by Rayleigh–Gans theory can be shown to depend on wavevector  $q$  as

$$I_{\text{VH}}(q)/I_{\text{VH}}(q = 0) = 1 - c_{\text{VH}}(qR)^2/5 + \mathcal{O}((qR)^4) \quad (6)$$

in the Guinier regime, with a prefactor  $c_{\text{VH}} = \Delta\varepsilon/\Delta\tilde{\varepsilon}$  in the  $q^2$  term for a homogeneous director field. The value of the parameter  $c_{\text{VH}}$  determined from a fit of equation (6) to the measured depolarized intensities (see figure 2) can be then be compared with  $\Delta\varepsilon/\Delta\tilde{\varepsilon}$  obtained from the depolarization ratio (equation (2)).

For the unpolymerized particles, we obtain  $c_{\text{VH}} = 1.44$ , which is in reasonable agreement with the value  $\Delta\varepsilon/\Delta\tilde{\varepsilon} = 2.41$ , given the uncertainty in the effective ordinary dielectric constant  $\tilde{\varepsilon}_{\perp}$  which is due to the unknown director field inside the particles. For the polymerized particles, the value  $c_{\text{VH}} = 0.265$  agrees similarly well with the value  $\Delta\varepsilon/\Delta\tilde{\varepsilon} = 0.155$  obtained from the depolarization ratio.

Characterization of unpolymerized particles by electron microscopy is hampered by the particles' melting in the electron beam. Under normal treatment, however, the weak charge on the unpolymerized particles allows them to be kept over many months at volume fractions of some percent without irreversibly aggregating.

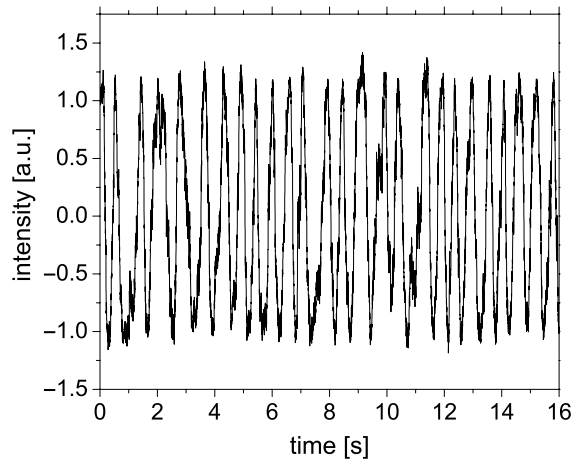


**Figure 3.** Brightness of microscope images of a birefringent particle spinning in a circularly polarized optical trap, viewed under crossed polarizers as a function of time. We used broadband light with wavelengths between 610 and 700 nm to produce the images. The brightness was measured at the centre of the microscope image of the particle which was determined with a centre-finding algorithm. The frequency of the rotation is  $\Omega \approx 1.83$  Hz. Negative values of the intensity are due to the subtraction of the background intensity which was present due an infrared background from the illumination source.

Birefringent particles with sizes of some micrometres can also be observed directly in an optical microscope. When viewed under crossed polarizers, the particles appear as spots whose brightness fluctuates as they rotate due to Brownian motion. When the particles have sizes of a few micrometres, their internal nematic structure can be deduced from the intensity pattern under crossed polarizers. Upon rotation of the particles we observe a transition from a baseball-type to a Maltese-cross pattern, indicating that at least for the larger nematic particles the director configuration is bipolar, consistent with the results of Cairns *et al* [12]. Large particles can also be efficiently trapped with tightly focused laser beams delivered through the microscope objective. Placing a quarter-waveplate in the laser beam before it enters the microscope objective, the polarization of the optical tweezer beam becomes, say, right-circular with a power  $P_+$ , and the birefringent particle experiences a constant torque pointing along the laser beam, due to the transfer of photon angular momentum to the particle [18, 19] and a counteracting viscous torque due to the solvent viscosity  $\eta$ . Figure 3 shows the brightness of a birefringent particle as it performs several rotation cycles. The brightness roughly follows a  $\sin^2(\Omega t)$  dependence with a constant rotation frequency  $\Omega$  given by the balance of the viscous rotational drag torque  $8\pi\eta a^3\Omega$  with the optical torque  $(P_+ - P'_+)/\omega$ . Here  $P'_+$  is the power in the right-circular component after passage through the birefringent particle [20].

Images of the intensity patterns observed under crossed polarizers are shown in figure 4. These patterns show a quite complex shape with a bright centre whose intensity is modulated as the particle rotates. This pattern is quite in contrast to the baseball or Maltese-cross patterns observed for very large particles which can be understood by geometrical optics [21]. However, its precise origin is not known at present.

Besides their use for studying the coupling between rotation and translation mediated by HI [22], such birefringent particles could be used as probes for local deformations in complex materials such as polymer gels or cells, complementarily to conventional microrheology where the displacements of single particles [23] or displacement correlations between two particles [24] are used to map deformation fields or local viscoelastic properties.

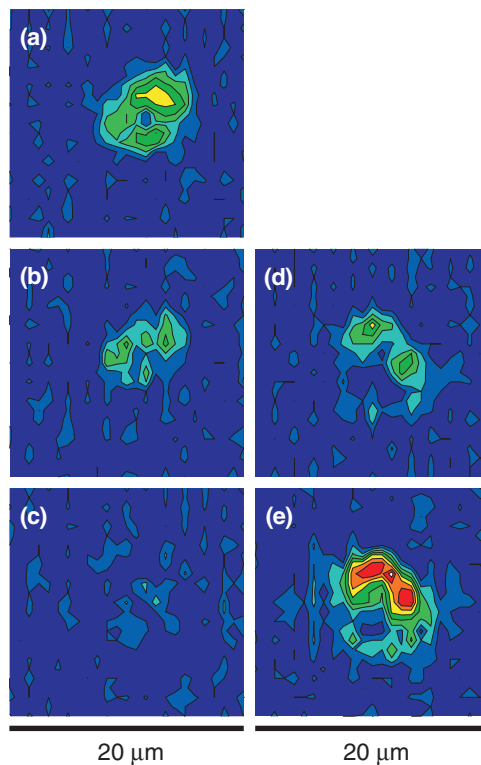


**Figure 4.** Microscope images of a birefringent particle spinning in a circularly polarized optical trap viewed under crossed polarizers. Images were taken at phase angles  $\tilde{\varphi} = -\pi/4$  (a),  $-\pi/8$  (b), 0 (c),  $\pi/8$  (d) and  $\pi/4$  (e). Red denotes highest, and dark blue lowest intensity. When the optical axis of the particle is parallel to the polarizer (c) the transmission is minimal. The asymmetry of the images around the phase angle  $\tilde{\varphi} = 0$  and the apparent tilting of the particle axis between (a) and (d) are due to an oblique incidence of the trapping beam.

In summary, we have reported on the preparation and characterization of highly birefringent mesogen particles. We have presented preliminary results on using these particles as probes for studying the coupling of rotational and translational motion by hydrodynamic interactions, using polarization microscopy.

### Acknowledgments

We thank M Reichert and A Mertelj for fruitful discussions. This work is funded by the Transregio-Sonderforschungsbereich 6 ‘Colloidal Dispersions in External Fields’. HS is supported by a Heisenberg Fellowship of the Deutsche Forschungsgemeinschaft.

### References

- [1] Russel W B and Saville D A 1989 *Colloidal Dispersions* (Cambridge: Cambridge University Press)
- [2] Pusey P N 1991 Colloidal Suspensions *Liquids, Freezing and Glass Transition* ed J P Hansen, D Levesque and J Zinn-Justin (Amsterdam: North-Holland) p 763
- [3] Dhont J K G 1996 *An Introduction to the Dynamics of Colloids* (Amsterdam: Elsevier)
- [4] Degiorgio V, Piazza R and Jones R B 1995 *Phys. Rev. E* **52** 2707



- [5] Mertelj A, Arauz-Lara J L, Maret G, Gisler T and Stark H 2002 *Europhys. Lett.* **59** 337
- [6] Koenderink G H, Zhang H, Lettinga M P, Nägele G and Philipse A P 2001 *Phys. Rev. E* **64** 022401
- [7] Kanetakis J, Tölle A and Sillescu H 1997 *Phys. Rev. E* **55** 3006
- [8] Degiorgio V, Piazza R, Bellini T and Visca M 1994 *Adv. Colloid Interface Sci.* **48** 61
- [9] Piazza R and Degiorgio V 1992 *Physica A* **182** 576
- [10] Bishop A I, Nieminen T A, Heckenberg N R and Rubinsztein-Dunlop H 2004 *Phys. Rev. Lett.* **92** 198104
- [11] Umbanhowar P B, Prasad V and Weitz D A 2000 *Langmuir* **16** 347
- [12] Cairns D R, Eichenlaub N S and Crawford G P 2000 *Mol. Cryst. Liq. Cryst.* **352** 275
- [13] Bohren C F and Huffman D R 1983 *Absorption and Scattering of Light by Small Particles* (New York: Wiley)
- [14] Loiko V A and Molochko V I 1999 *Appl. Opt.* **38** 2857
- [15] Stark H and Gisler T 2004 unpublished
- [16] Žumer S and Doane J W 1986 *Phys. Rev. A* **34** 3373
- [17] Kerker M 1969 *The Scattering of Light and Other Electromagnetic Radiation* (New York: Academic)
- [18] Beth R A 1936 *Phys. Rev.* **50** 115
- [19] Friese M E J, Nieminen T A, Heckenberg N R and Rubinsztein-Dunlop H 1998 *Nature* **394** 348
- [20] Nieminen T A, Heckenberg N R and Rubinsztein-Dunlop H 2001 *J. Mod. Opt.* **48** 405
- [21] Drzaic P S 1998 *Liquid-Crystal Dispersions* (Singapore: World Scientific)
- [22] Reichert M and Stark H 2004 *Phys. Rev. E* **69** 031407
- [23] Mason T G and Weitz D A 1995 *Phys. Rev. Lett.* **74** 1250
- [24] Crocker J C, Valentine M T, Weeks E R, Gisler T, Kaplan P D, Yodh A G and Weitz D A 2000 *Phys. Rev. Lett.* **85** 888